energy&fuels

Article

Cite This: Energy Fuels XXXX, XXX, XXX−XXX

pubs.acs.org/EF

Phase Envelopes for Reservoir Fluids with Asphaltene Onset Lines: An Integral Computation Strategy for Complex Combinations of Two- and Three-Phase Behaviors

Martin Cismondi*

Instituto de Investigación y Desarrollo en Ingeniería de Procesos y Química Aplicada (IPQA), Universidad Nacional de Córdoba (UNC)−Consejo Nacional de Investigaciones Científicas y Técnicas de la República Argentina (CONICET), Avenida Velez Sarsfield 1611, Ciudad Universitaria, X5016GCA Córdoba, Argentina

ABSTRACT: Despite the fact that many publications have dealt with asphaltene onset pressure (AOP) lines during the last 2 or 3 decades, no explicit method for tracing these and other related boundaries from equation of state (EoS) models has been proposed in the literature. In this work, a new integral algorithmic strategy for the construction of complete phase envelope diagrams based on an EoS is presented. The method of Michelsen for tracing two-phase boundaries is used, while for three-phase saturation lines, an equivalent method was designed, including a second set of *K* factors and a phase fraction as extra independent variables. The double-saturation point is defined, and its importance is highlighted, from both phase behavior and algorithmic perspectives. Specific issues as recognition of unstable segments, such as false bubble curves, are also discussed. Three different fluids from the literature are taken as case studies to illustrate the application of the proposed strategy and discuss different types of behavior. In particular, an unexpected second three-phase region was predicted at higher temperatures in two of the three cases studied. This could serve as inspiration for new experimental studies, to see whether the existence of such a region can be confirmed for some reservoir fluids, or it could be just an artificial behavior predicted by the models. In summary, computer codes based on the proposed strategy might become a useful tool for researchers or professionals dealing with asphaltene phase behavior in reservoir fluids.

1. INTRODUCTION

Regardless of their cubic or statistical association fluid theory (SAFT) nature, equations of state (EoS) have been used to model asphaltene phase behavior in reservoir fluids for at least 2 decades already. The importance of the upper and lower asphaltene onset pressures (AOPs) is widely recognized in the literature, where many studies of either experimental or modeling character are available, with different approaches. See for example Chapter 12 in the book by Pedersen and Christensen[1] and the recent works by Arya et al.[2,3] for introductory reviews.

In terms of algorithms or calculation methods, details are rarely provided in publications. However, on the basis of the experience of the author and communications with colleagues, most studies normally resorted, inefficiently, to a series of two- and multi-phase flashes. Moreover, that could be one of the reasons why some modeling simplifications are often used, for example, that only asphaltenes are allowed to partition between the liquid phases and no other component can enter the asphaltenic phase, considered to be made of pure asphaltenes.[4,5] Surprisingly, no explicit method for tracing different phase boundaries, such as AOP lines and the intermediate three-phase bubble line, is found in the literature (the reader not familiar with these curves might find it useful to have a look at Figures 2 and 6). Neither can we find previous publications devoted to studying the different possible behaviors, i.e., how these and other related segments can arrange in the complete phase envelope of a specific asphaltenic reservoir fluid, as predicted by a model.

In this work, a new integral algorithmic strategy for the construction of complete phase envelopes based on an EoS will be proposed and implemented. As usual in the literature, the asphaltenic phase is formally treated as a dense liquid, and all compounds are allowed to enter all phases; i.e., there are no compositional simplifications or restrictions. Every curve is treated as the boundary of either a two- or three-phase region in the pressure−temperature diagram for a specific fluid. In other words, every point along these lines determines the $T-P$ conditions where an incipient phase appears or disappears. An important and interesting reference, to which the present work could be considered equivalent or similar in certain aspects, is the one by Lindeloff and Michelsen for hydrocarbon−water mixtures.[6] Despite some similarities in the general objectives and in the ways to formulate and solve the calculations, the main differences come naturally from the different phase behaviors and related diagrams involved in each case. Besides that, the general strategy proposed here for constructing the complete phase envelope of a fluid, to be discussed in section 2.2, is different, with the advantage of saving the stability tests, which can imply important computation times.

1.1. Double-Saturation Points and Their Role in Complete Phase Envelope Diagrams.

First of all, it is

Special Issue: 18th International Conference on Petroleum Phase Behavior and Fouling

Received: September 18, 2017
Revised: December 15, 2017

DOI: 10.1021/acs.energyfuels.7b02790
Energy Fuels XXXX, XXX, XXX−XXX

important to realize that, from a phase behavior or calculation point of view, upper AOP lines are two-phase boundaries, just like typical bubble or dew lines but involving liquid−liquid (L−L) separation, while special bubble lines for these systems (in the presence of two liquid phases) and lower AOP lines are both three-phase boundaries.

Before discussing a general strategy for constructing complete phase envelopes containing both two- and three-phase boundaries, such as these different lines of interest for asphaltenic systems, it is convenient to pay attention to a special point, which is characteristic of these types of phase behavior. This point, marking the ends of different two-phase boundaries and the beginning of a three-phase region, has been referred to by Michelsen as intersections between phase boundaries or a three-phase point with two incipient phases (see for example Chapter 12, section 4 in the book by Michelsen and Møllerup[7]). In this work, to be more explicit and concise, this type of point will be referred to as a double-saturation point, because it indicates conditions at which two different new incipient phases may start to form and separate at the same time from a homogeneous saturated fluid.

The following sections are dedicated first to describe the method for tracing three-phase boundaries and then to discuss the general strategy to identify the double-saturation points and, depending upon them, organize the calculation of the different lines that will be present in each specific case.

2. METHODOLOGY

2.1. Calculation Method for Three-Phase Boundaries. As suggested by Michelsen and Møllerup,[7] the principles used for calculating phase boundaries for a two-phase region are extended here to the calculation of three-phase boundaries by introducing as new variables an additional set of K factors and a phase fraction β for the phase split between the two phases, which are present at both sides of the boundary. The notation will be established for the case of a three-phase bubble line, but the method and the corresponding code can be easily adapted for a line where the incipient phase is a liquid, e.g., the lower AOP line.

The three phases that need to be considered are a vapor, a hydrocarbon liquid, and an asphaltene-rich phase. They are denoted as V, L, and L2, with molar fractions y_i, x_i, and w_i, respectively. The L phase is chosen as the reference phase for defining the two sets of K factors, which results in

$$K_i = y_i/x_i \tag{1}$$

for the standard vapor−liquid separation and

$$K_i^s = w_i/x_i \tag{2}$$

for the liquid−liquid separation, with a fraction β for phase L2.

With N being the number of components, the resulting system has $2N + 3$ independent variables and $2N + 2$ equations. After completion with the specification equation, we have the following vectors of variables X and equations F to be solved:

$$X = \begin{bmatrix} \ln K_1 \\ \cdots \\ \ln K_N \\ \ln K_1^s \\ \cdots \\ \ln K_N^s \\ \ln T \\ \ln P \\ \beta \end{bmatrix} \quad F = \begin{bmatrix} \ln K_1 + \ln \hat{\phi}_1^{\mathrm{V}} - \ln \hat{\phi}_1^{\mathrm{L}} \\ \cdots \\ \ln K_N + \ln \hat{\phi}_N^{\mathrm{V}} - \ln \hat{\phi}_N^{\mathrm{L}} \\ \ln K_1^s + \ln \hat{\phi}_1^{\mathrm{L2}} - \ln \hat{\phi}_1^{\mathrm{L}} \\ \cdots \\ \ln K_N^s + \ln \hat{\phi}_N^{\mathrm{L2}} - \ln \hat{\phi}_N^{\mathrm{L}} \\ \sum_{i=1}^{N} (y_i - x_i) \\ \sum_{i=1}^{N} (w_i - x_i) \\ X_S - S \end{bmatrix} \tag{3}$$

Note that, on the basis of material balances and eqs 1 and 2, each new set of K_i, K_i^s, and β values can be translated into the corresponding sets of mole fractions through the following equations:

$$x_i = z_i/(1 - \beta + \beta K_i^s) \tag{4}$$

$$y_i = K_i x_i \tag{5}$$

$$w_i = K_i^s x_i \tag{6}$$

For a computational implementation, eqs 4−6 also need to be taken into account when writing the elements of the Jacobian, i.e., the derivatives of each F in eq 3 with respect to each X. Note for example that, except for the last specification equation, all F functions will have non-zero derivatives with respect to β.

After convergence of a first point by a full Newton's method, the Jacobian is used to calculate the vector of sensitivities of the solution, which, in turn, will provide excellent initialization for a subsequent point. In this way, the construction of the three-phase boundary can proceed smoothly. Details for the implementation of these numerical strategies for tracing highly nonlinear hyperlines, often known as continuation methods, have been given by Michelsen[7,8] for the case of multicomponent two-phase boundaries. Additional and complementary explanations have been provided for example by Cismondi et al. for the cases of azeotropic lines and isobaric or isothermal diagrams in azeotropic binary systems.[9]

What is crucial for the application of these methods in general and specially for the three-phase boundaries considered in this work is the availability of good initial estimates for a first point. An ideal starting point would be a double-saturation point, from each of which two different three-phase boundary lines, with different incipient phases, will depart. The algorithmic strategy for detecting these double-saturation points and organizing the calculation of complete phase envelopes in different behaviors is discussed in the next section.

2.2. Methodology: General Algorithmic Strategy. A natural strategy, following Michelsen's typical approaches,[7,6] could start with the calculation of a two-phase boundary, testing each point for stability. When this line becomes unstable, that is an indication that a double-saturation point has been just passed. An alternative strategy, instead, can start from calculating different two-phase boundaries but saving the stability analysis and then detecting intersections between the different boundaries. Each intersection means a double-saturation point, from which the unstable portion of each line can be discarded afterward. The design of an alternative strategy like this, in a way analogous to the strategies proposed by Cismondi and Michelsen in the construction of different phase diagrams for binary systems,[9−12] requires an *a priori* analysis and, at least preliminary, classification of the different behaviors that can be found.

The specific strategy proposed and implemented in this work involves the following stages: (1) calculation of the two-phase envelope starting from a dew point at low pressure, (2) calculation of a second two-phase envelope section, starting from (a) low T

DOI: 10.1021/acs.energyfuels.7b02790
Energy Fuels XXXX, XXX, XXX−XXX

Table 1. Selected Fluids for Illustration of the Methodology Developed

	case 1	case 2	case 3
experimental	Burke et al.[14]	Jamaluddin et al.[15]	Jamaluddin et al.[16] fluid A
characterized	Gonzalez et al.[4]	Pedersen and Christensen[1]	Pedersen and Christensen[1]
pseudo-compounds	8	16	15
EoS	PR78[17]	SRK[18]	PR76[19]

bubble point (if the first line diverged to high P) or (b) high P L−L saturation point (if the first line ended at low T as a bubble line), (3) detect double-saturation points as intersections between two-phase boundary segments and discard unstable portions of the two-phase boundaries previously generated, and (4) calculate the two three-phase boundaries, departing from each double-saturation point.

The numerical initialization for the first point along each three-phase boundary is based on the approximate coordinates of the double-saturation point, which were, in turn, estimated by a linear interpolation between the closest two-phase boundary calculated points, after an intersection was detected (step 3). The specification for the first point is $\beta = 0$ (which defines a double-saturation point), and convergence required 2 Newton steps for each of these calculations performed in this work.

In the case that no intersection is detected in step 3, it means that the whole inner two-phase boundary is unstable and has to be discarded. Then, the starting points for two different three-phase boundaries, corresponding to the (three-phase) bubble line and the lower AOP line, need to be found independently. For the first one, an initial three-phase bubble point can be detected at some specified low temperature as follows. The pressure of the converged false bubble point, calculated as a simple saturation point, will normally serve as an excellent initialization if complemented with reasonable separation factors between the two liquid phases. Our recommendation for the initialization of such separation factors is the following:

$$K_i^S = \frac{\hat{\varphi}_i^{\mathrm{F}}}{\hat{\varphi}_i^{\mathrm{Asp}}} \tag{7}$$

where the superscripts F and Asp stand for the feed or original fluid (the liquid in the false bubble point) and a pure asphaltene phase, respectively.

Then, to find a lower AOP, where the incipient phase is the asphaltene-rich phase, the search is based on finding T−P conditions where the fugacity of the pure asphaltene pseudo-compound equals its fugacity in a standard vapor−liquid flash at the same conditions. This will provide good initial estimates for the calculation of the first lower AOP point. The search can start at a fixed low temperature, e.g., that of the first calculated three-phase bubble point and half the pressure. If the fugacity is lower in the pure form, then the pressure is reduced. If this persists at 1 bar, then pressure is fixed and a higher temperature at which the equality indicated above is fulfilled can be reached for example by the secant method.

The stop criteria for terminating the computation of each three-phase boundary line can be based on a variety of situations. First, the classic conditions of the temperature going below (or the pressure exceeding) a preset value, e.g., 150 K or 2000 bar, or when the number of iterations exceeds another high preset value, which means numerical problems preventing convergence. Specifically for three-phase boundaries, another reasonable condition for termination is $\beta < 0$, which implies the disappearance of a phase. This can occur when, after describing a closed path, the line returns to the original double-saturation point and the continuation of mathematical solutions leads to cross it, jumping to the other side of the line. This other side of the three-phase boundary line will be associated with negative flashes,[13] i.e., distribution of phases fulfilling the isofugacity condition but not the material balance for the global composition being considered.

3. RESULTS AND DISCUSSION

For illustration of the proposed methodology, three different fluids leading to three different types of complete diagrams were selected from the literature. References and some basic details are given in Table 1.

It has to be stressed that no modeling decisions were taken in this work. In other words, we used the same models and characterizations of the fluids as indicated by the authors in the original modeling works, to reproduce their results and go beyond, to unveil the complete predicted diagrams. These complete diagrams, presented in this section, include regions and double-saturation points that were not shown previously by the corresponding authors. In case 1, the work by Gonzalez et al.[4] had a different focus, and not even a segment of an AOP line was presented in that publication. Nevertheless and despite the simplification made by the authors considering the asphaltene-rich phase to be composed of pure asphaltenes, the diagram presented here is consistent with the occurrence of upper and lower AOPs at 373 K, as reported for this fluid by Burke et al.[14]

The upper part of Figure 1 presents, for case 1, what results after steps 1 and 2 of the general strategy discussed in the previous section. These are two different continuous sets of solutions to classic two-phase boundary calculations: one started from the bubble side and the other from the dew side, including not only the stable but also the unstable portions of these boundaries. The lower part shows the result of the complete procedure, i.e., the complete and stable phase envelope diagram predicted by the model, including the different one-, two-, and three-phase regions. According to the complete diagram shown in Figure 1, the upper and lower AOP curves meet at a double-saturation point, together with the three-phase bubble curve, around 445 K and 225 bar. A restricted portion of the same diagram is presented with more detail in Figure 2, including a rather typical range of conditions at which the precipitation of asphaltenes is studied. In addition, the boundaries known as upper and lower AOP as well as the phases present in each region are explicitly identified.

Coming back to Figure 1, note that there is also a second double-saturation point, located around 780 K and 125 bar, from where a second, high-temperature three-phase region starts. This opens a question about whether this second three-phase region, with specific boundaries associated, actually exists for real fluids. The discussion might be of very low practical relevance for typical upstream applications, and in view of the thermal degradation that the fluid may suffer in the temperature range involved, one may think that it does not deserve attention, not even from a purely scientific point of view. However, there have been some interesting experimental findings reported in the literature that we should considered here. Cartlidge et al. investigated the phase behavior of Athabasca bitumen vacuum bottoms (ABVB) + n-dodecane + hydrogen mixtures at temperatures and pressures ranging up to 725 K and 7 MPa using an X-ray view cell.[20] The preliminary phase diagram that they presented in Figure 1 for a specific mixture suggests a LLV region extending up to around 750 K. In a later work, also by the group of Shaw,[21] the effects of both reversible phase behavior and irreversible thermolysis con-

DOI: 10.1021/acs.energyfuels.7b02790
Energy Fuels XXXX, XXX, XXX−XXX

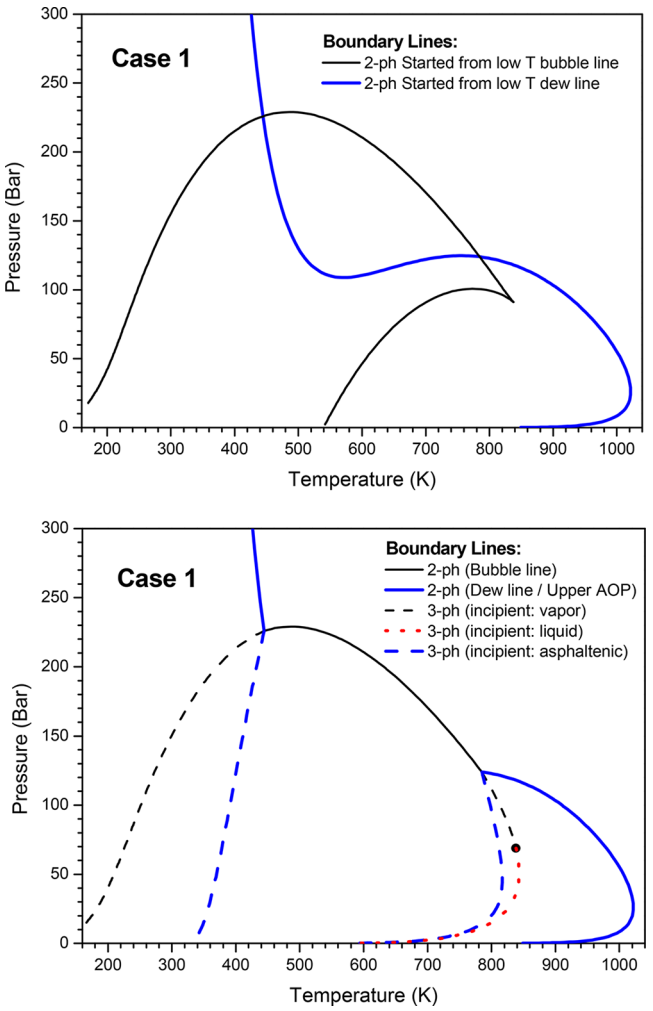

Figure 1. Calculated two-phase boundaries, including unstable segments (upper part) and complete phase envelope obtained with the proposed algorithmic strategy (lower part), for case 1 defined in Table 1. The black dot is a calculated critical point along one of the three-phase boundaries.

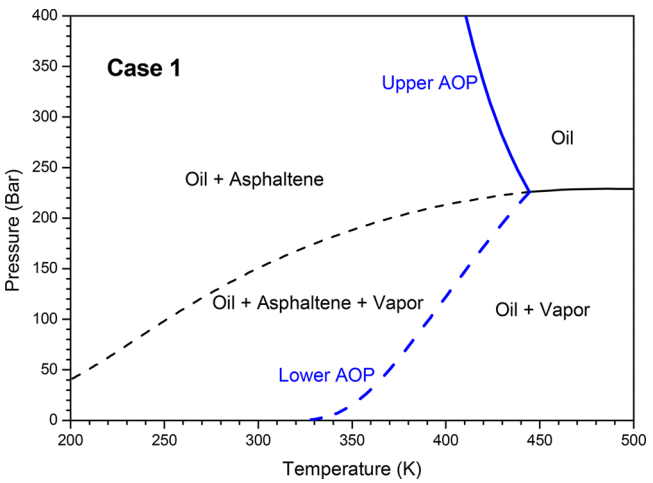

Figure 2. Detailed zoom of the lower part of Figure 1, in the range of practical interest for case 1, indicating the lines of AOPs and the different regions with one, two, and three stable phases.

ditions on the rejection of the inorganic fractions of ABVB were studied at high temperatures up to 380 °C. One of the different interesting findings was that, even when thermal degradation occurs, the phase behavior of the system is not much affected.[21] Therefore, it might well be that, in the case that it actually occurs for some real asphaltenic fluids, a three-phase behavior, such as the one predicted for the high-temperature region in Figure 1, could be detected experimentally. Moreover, Table 3 in the work by Cartlidge et al. presented a list of technologies for heavy oil upgrading, operating at high temperatures, which, in some cases, may reach values above 800 K.[20] Then, the LLV regions under discussion might be something not only interesting in terms of phase behavior, as far as we know not previously reported in the literature, but also important to consider for a proper design or optimization of high-temperature technologies, such as those for heavy oil upgrading.

The complete phase envelope diagram for case 2 is presented in Figure 3. Note here that the behavior is qualitatively very similar to the behavior observed for case 1, again with two different double-saturation points, but now closer to each other. The high-temperature region where an asphaltene-rich phase

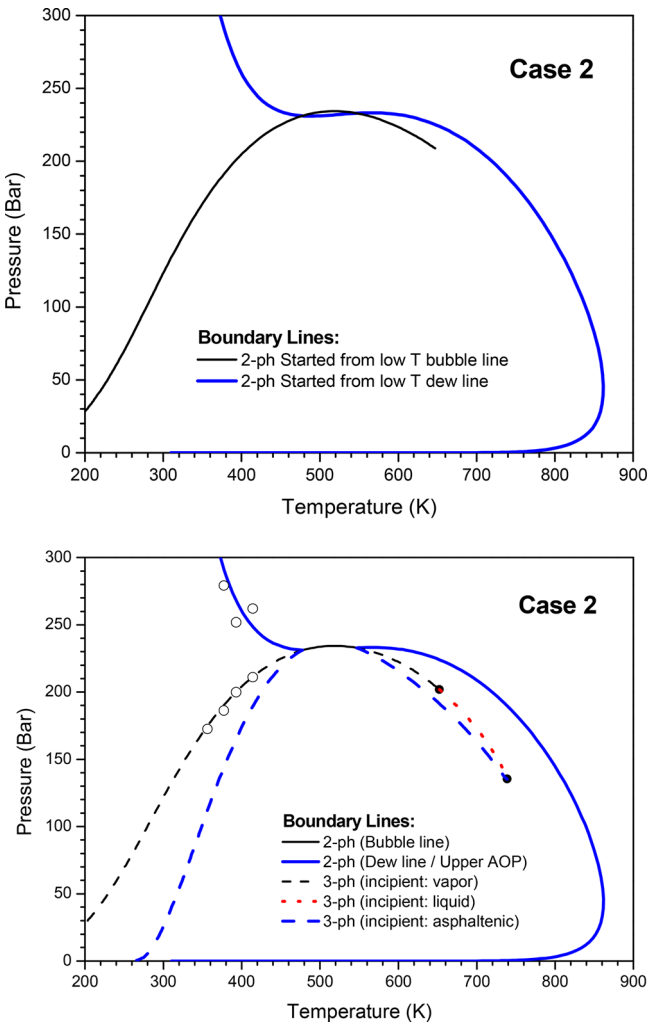

Figure 3. Calculated two-phase boundaries, including unstable segments (upper part) and complete phase envelope obtained with the proposed algorithmic strategy (lower part), for case 2 defined in Table 1. Black dots are calculated critical points along one of the three-phase boundaries. Empty circles indicate experimental upper AOPs and bubble points reported by Jamaluddin et al.[15]

DOI: 10.1021/acs.energyfuels.7b02790
Energy Fuels XXXX, XXX, XXX−XXX

separates again could have more practical importance in this case, starting at around 540 K based on the predicted diagram. This can provide good motivation or incentive for new experimental studies devoted to confirm the existence of such a second three-phase region at high temperatures. It does not mean that we should trust quantitatively the high-temperature predictions presented for these fluids, because they are based on simple characterizations and parameters obtained by fitting limited data in the lower temperature range. However, at least qualitatively, predictions suggest the possibility of existence of such high-temperature three-phase regions for these or other similar fluids. In that sense, the construction of complete complex phase envelopes, such as the envelopes presented in this work, when the modeling is based on fitting some available data, could be useful to orientate further experimental studies at higher temperature ranges.

Returning to Figure 3, note also that, despite the similarities, there is one clear qualitative difference between the diagrams obtained for cases 1 and 2: the high-temperature and high-pressure three-phase region closes itself (around 130 bar and 740 K) in case 2, while it continues toward very low pressures in case 1 without closing. Of particular interest, at least in terms of phase behavior understanding, is the fact that the closed three-phase boundary in case 2 contains all three possible types of boundaries, each one characterized by a different incipient phase, with two critical points setting the limits or transitions between them. To fix ideas and provide some basic guidance for the interpretation of this complex predicted region, let us take the path across this closed three-phase boundary, considering the implications of each point that we find on the way. Starting at the double-saturation point at 546.6 K and 232.9 bar, it implies a saturated oil phase with a first bubble appearing simultaneously with a first drop of an asphaltenic phase. As we move to higher temperatures along the black dashed line, the quantity or fraction of the asphaltenic phase increases, while vapor continues to be the incipient phase. As we continue in the same direction, the composition and properties of such a vapor phase become closer and closer to the oil phase, until they become indistinguishable at the first critical point, located at 652.4 K and 201.8 bar. Once the critical point is crossed, the incipient phase is the oil, and most of the system is in the state of a dense vapor phase, except for a certain quantity of the asphaltenic phase as before. Note that we had to change the label of the phase present in a larger quantity from oil to vapor, but its properties change continuously and independently of names, just as happens across a standard critical point on a simple and classic two-phase envelope. As we continue along the red dotted line, the incipient oil phase will differentiate more and more from the vapor phase and, on the contrary, will approach the characteristics of the aphaltenic phase, until they are the same when the second critical point is reached at 738.9 K and 135.3 bar. Once on the blue dashed line, the incipient phase will be the aphaltenic phase, while the saturated system distributes itself between an oil phase and a vapor phase. As we continue and return to the starting point, the oil phase fraction increases, with lower and lower contents of asphaltenes, while the vapor phase fraction decreases progressively until disappearing at the double-saturation point. All of these changes can also be followed and confirmed in Figure 4, which presents the evolution of methane and asphaltene mole fractions in the three phases along these boundaries versus pressure.

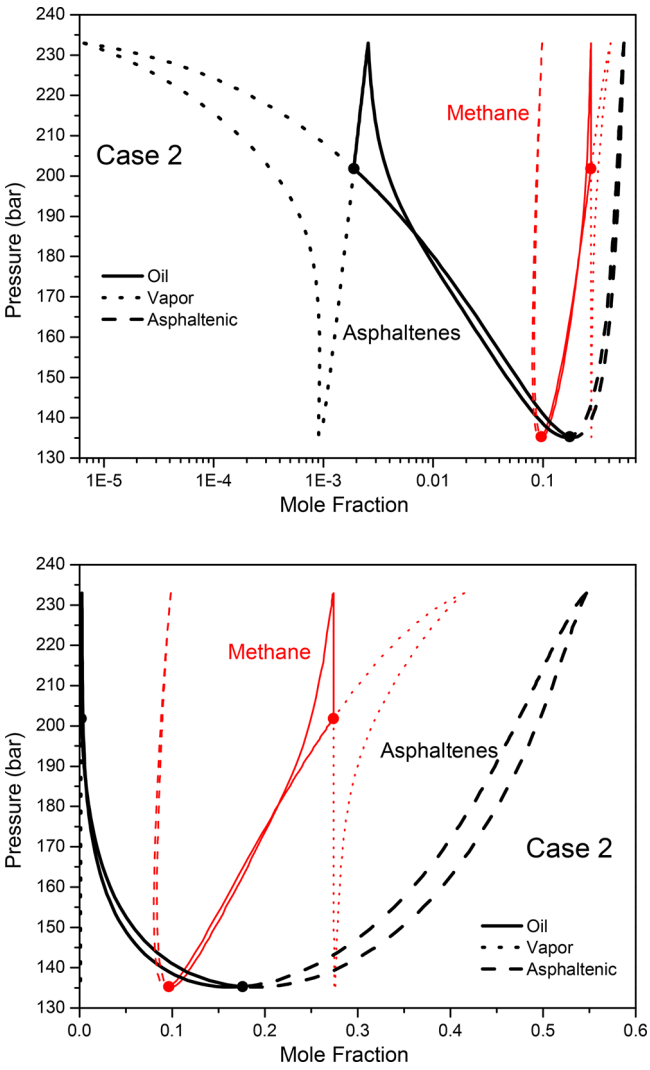

Figure 4. Methane and asphaltene mole fractions along the calculated closed three-phase boundary in the higher temperature region of Figure 3 for case 2. The same information is presented in both log and linear scales for mole fractions, to better appreciate the different curves.

Finally, the diagram obtained for case 3 is shown in Figures 5 and 6. Contrary to the previous cases, not even a single double-saturation point appears. In other words, the different boundaries do not touch or intersect each other. This new behavior can be seen as related to the behavior observed for case 1 but now with the two previously separated regions having merged into a single continuous three-phase region. Furthermore, the transition from the behavior observed for case 1 to the behavior observed for case 3 would imply a special point where the two double-saturation points, observed for case 1, merge into one. In other words and from a different perspective, the three curves present in case 3 would touch each other tangentially at such a singular point. Although a deeper analysis of transitions like that is beyond the scope of the present work, it is interesting to realize how the different behaviors encountered can be related and how one of them could be probably transformed into another by changes of either composition or parameter values.

A final comment will be dedicated to bubble lines. It should be clear, to everyone working with this type of systems, that, in

DOI: 10.1021/acs.energyfuels.7b02790
Energy Fuels XXXX, XXX, XXX−XXX

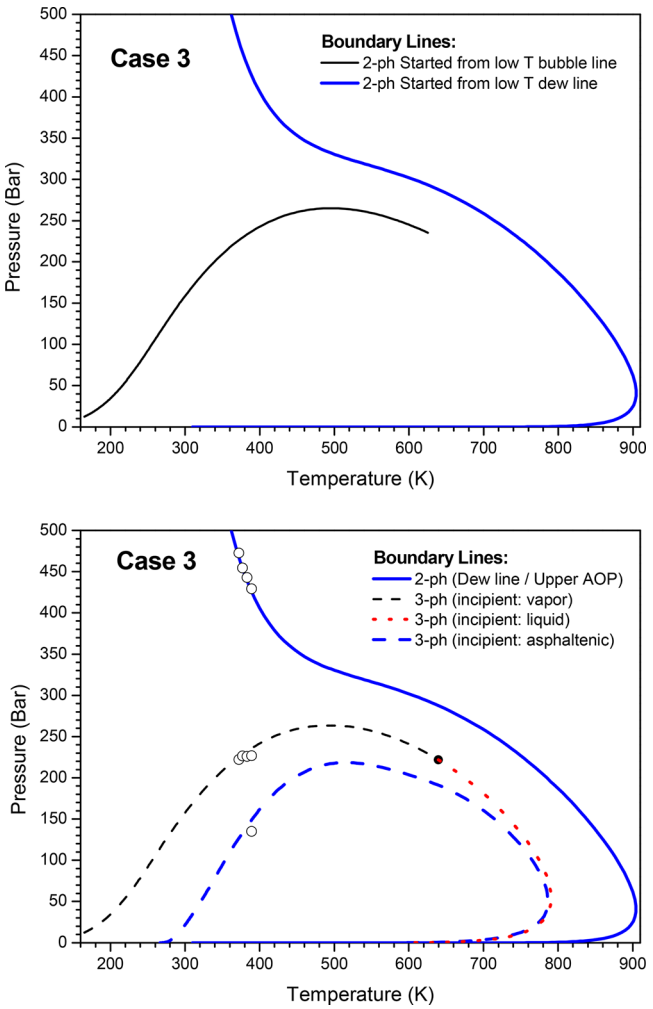

Figure 5. Calculated two-phase boundaries, including unstable segments (upper part) and complete phase envelope obtained with the proposed algorithmic strategy (lower part), for case 3 defined in Table 1. The black dot is a calculated critical point along one of the three-phase boundaries. Empty circles indicate experimental upper and lower AOPs as well as bubble points reported by Jamaluddin et al.[16]

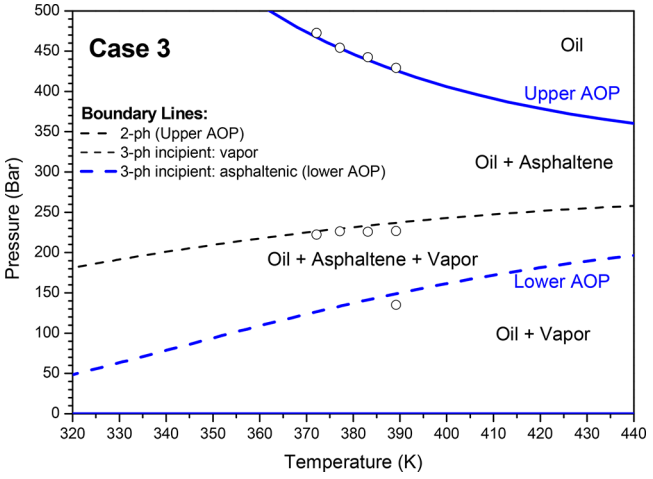

Figure 6. Detailed zoom of the lower part of Figure 5, in the range of practical interest for case 3, indicating the lines of AOPs and the different regions with one, two, and three stable phases.

the presence of a segregated asphaltenic phase, a bubble point is part of a three-phase boundary. Nevertheless, sometimes bubble lines are calculated using standard procedures for two-phase boundaries, which are rigorously unstable in these fluids, with asphaltenes or other substances forming a second liquid phase before the appearance of the vapor phase. Most publications do not clarify this and do not provide details regarding the calculation methods used either. In many cases, the difference between the three-phase bubble line and the unstable two-phase bubble line can be quite low in the pressure−temperature diagram, sometimes negligible. This can be observed for cases 2 and 3 in Figure 7, which present both

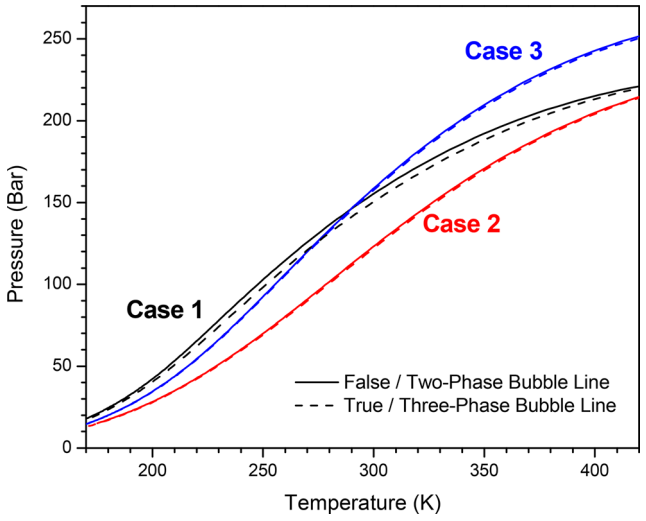

Figure 7. Comparison between false and true bubble lines for the three cases considered in this work.

curves for each of the cases illustrated and discussed in this work. Note, however, that the difference can be important for case 1, reaching values of around 5 bar in the intermediate range, including ambient temperatures.

4. CONCLUSION

An integral strategy for the automated construction of complete envelopes containing two- and three-phase boundaries was developed and successfully implemented for different asphaltene case studies.

Although cubic EoS were used for these cases, following the original modeling and characterization by other authors, it is important to remark that the proposed methods are equally applicable to any type of EoS, e.g., SAFT as well.

From the cases analyzed, it becomes clear that different types of behavior can be encountered when the complete phase diagram is considered for a given reservoir fluid. For example, dependent upon the case, the upper and lower AOP curves may or may not converge, together with the three-phase bubble curve, to a double-saturation point. A classification of the different possible behaviors and a better understanding of the transitions between them would definitely require further work in that direction.

AUTHOR INFORMATION

Corresponding Author

*E-mail: martin.cismondi@gmail.com and/or martin.cismondi@unc.edu.ar.

DOI: 10.1021/acs.energyfuels.7b02790
Energy Fuels XXXX, XXX, XXX−XXX

ORCID
Martin Cismondi: 0000-0002-9349-8594

Notes
The author declares no competing financial interest.

■ ACKNOWLEDGMENTS

The author acknowledges the financial support received from the following Argentinean institutions: Consejo Nacional de Investigaciones Científicas y Técnicas de la República Argentina (CONICET), Agencia Nacional de Promoción Científica y Tecnológica (ANPCyT), and Universidad Nacional de Córdoba (UNC).

■ REFERENCES

(1) Pedersen, K. S.; Christensen, P. L. *Phase Behavior of Petroleum Reservoir Fluids*; CRC Press (Taylor & Francis Group): Boca Raton, FL, 2006; DOI: 10.1201/9781420018257.
(2) Arya, A.; Liang, X.; Von Solms, N.; Kontogeorgis, G. M. *Energy Fuels* **2017**, *31* (2), 2063−2075.
(3) Arya, A.; Liang, X.; Von Solms, N.; Kontogeorgis, G. M. *Energy Fuels* **2017**, *31* (3), 3313−3328.
(4) Gonzalez, K.; Nasrabadi, H.; Barrufet, M. *J. Pet. Sci. Eng.* **2017**, *154*, 602−611.
(5) Sabbagh, O.; Akbarzadeh, K.; Badamchi-Zadeh, a.; Svrcek, W. Y.; Yarranton, H. W. *Energy Fuels* **2006**, *20* (7), 625−634.
(6) Lindeloff, N.; Michelsen, M. L. *SPE J.* **2003**, *8* (3), 298−303.
(7) Michelsen, M. L.; Møllerup, J. *Thermodynamic Models: Fundamentals & Computational Aspects*, 2nd ed.; Stenby, E. H., Ed.; Tie-Line Publications: Holte, Denmark, 2007.
(8) Michelsen, M. L. *Fluid Phase Equilib.* **1980**, *4* (1−2), 1−10.
(9) Cismondi, M.; Michelsen, M. L.; Zabaloy, M. S. *Ind. Eng. Chem. Res.* **2008**, *47* (23), 9728−9743.
(10) Cismondi, M.; Michelsen, M. *Fluid Phase Equilib.* **2007**, *259* (2), 228−234.
(11) Cismondi, M.; Michelsen, M. L.; Zabaloy, M. S. *Proceedings of the 11th European Meeting on Supercritical Fluids*; Barcelona, Spain, May 4−7, 2008.
(12) Cismondi, M.; Michelsen, M. L. *J. Supercrit. Fluids* **2007**, *39* (3), 287−295.
(13) Whitson, C. H.; Michelsen, M. L. *Fluid Phase Equilib.* **1989**, *53* (C), 51−71.
(14) Burke, N. E.; Hobbs, R. E.; Kashou, S. F. *JPT, J. Pet. Technol.* **1990**, *42* (11), 1440−1446.
(15) Jamaluddin, A. K. M.; Joshi, N.; Iwere, F.; Gurpinar, O. *Proceedings of the SPE International Petroleum Conference and Exhibition in Mexico*; Villahermosa, Mexico, Feb 10−12, 2002; DOI: 10.2118/74393-MS.
(16) Jamaluddin, A. K. M.; Joshi, N.; Joseph, M. T.; D'Cruz, D.; Ross, B.; Creek, J.; Kabir, C. S.; McFadden, J. D. *Proceedings of the Petroleum Society's Canadian International Petroleum Conference*; Calgary, Alberta, Canada, June 4−8, 2000.
(17) Robinson, D. B.; Peng, D. Y. *The Characterization of the Heptanes and Heavier Fractions for the GPA Peng−Robinson Programs*; Gas Processors Association (GPA): Tulsa, OK, 1978.
(18) Soave, G. *Chem. Eng. Sci.* **1972**, *27* (6), 1197−1203.
(19) Peng, D. Y.; Robinson, D. B. *Ind. Eng. Chem. Fundam.* **1976**, *15* (1), 59−64.
(20) Cartlidge, C. R.; Dukhedin-Lalla, L.; Rahimi, P.; Shaw, J. M. *Fluid Phase Equilib.* **1996**, *117* (1−2), 257−264.
(21) Zou, X.-Y.; Dukhedin-Lalla, L.; Zhang, X.; Shaw, J. M. *Ind. Eng. Chem. Res.* **2004**, *43* (22), 7103−7112.

DOI: 10.1021/acs.energyfuels.7b02790
Energy Fuels XXXX, XXX, XXX−XXX